A Detailed Failure Analysis of Vertically Suspended Diffuser Pump Caused by Hex Head Bolt Fracture: The Marine Service Condition

M.R. Etminanfar [1], M. S. Safavi *[2] , S. Masumi [3], S. Khanmohammadi [4], J. Seied-Hamzeh [5], J. Khalil-Allafi [6]

[1,2,3,4,6]Research Center for Advanced Materials, Faculty of Materials Engineering, Sahand University of Technology, Tabriz, P.O.Box: 51335-1996 Iran.

[5]Heavy Duty Pumps and Water Turbine Manufacture Company, PETCO, Tabriz, Iran

Abstract

Vertically suspended diffuser pumps play a significant role in the seawater cooling systems of the petro-chemical and refinery industries. The present work deals with providing a detailed analysis of mechanisms involved in the early failure of hex head bolt used in the vertically suspended diffuser pump framework, which has served three years in the marine condition. The morphological and microstructural characteristics of the failed bolt were evaluated by optical microscope, scanning electron microscope (SEM), spark-optical emission spectroscopy (spark-OES), and X-ray diffraction (XRD) methods. Besides, a microhardness test was performed to assess the mechanical properties of the samples. The results demonstrated the presence of Cr, Fe, Mn, and Si elements in the microstructure of failed bolt, which coincides with the composition of stainless steel (X5CrMnN17-8). While there exist sulfur and oxide inclusions in the parts close to the surface, no surface-related defects were detected in the central part. Moreover, the microstructural assay showed that the failed sample was composed of austenite-martensite micro-duplex structure. The microhardness values of regions close to the surface of the failed bolt were higher than that of the central part by ≈20 %, since there is higher martensite content. Fractography images revealed a brittle fracture mechanism in the parts close to the surface, while ductile fracture was observed at the center of the bolt. In general, the main factor governing the failure of the bolt can be attributed to the lack of precise control over the chemical composition of the bolt and the application of an inappropriate fabrication process.

Keywords: Failure; Hex head bolt; Vertically suspended diffuser pump; Fractography; Stainless steel.

1. Introduction

Vertically suspended, overhung, and between bearings pumps are known as three types of centrifugal pumps, which possess a driving engine/electrical motor located above the ground. As a simple definition, a vertical pump is a rotary apparatus that can receive the energy from the fluid and transform it into work. It can extract the fluids from the underground well or reservoir, e.g., water and oil. At least one rotating impeller, coupled with a shaft, has a duty to direct the fluid into the diffuser. Multiple impellers can be attached to the shaft if there is a need for pumping the fluids from deeper wells [1-3].

The vertical turbine pump bears a number of significant advantages over the horizontal one, as follows: (i) space-saving, (ii) eliminating the need

**Corresponding author*
Email:samansafavi1992@gmail.com
Address: : Research Center for Advanced Materials, Faculty of Materials Engineering, Sahand University of Technology, Tabriz, P.O. Box: 51335-1996 Iran.
1. Assistant Professor
2. Ph.D. Candidate
3. M.Sc. Student
4. M.Sc. Student
5. M.Sc.
6. Professor

for additional well supply pump, (iii) versatility in service medium, (iv) enduring lower wear due to the absence of radial thrust on the shaft, and (v) ability to preserve its capacity even with fluctuations in the head. Besides, there is no need to remove the air from the vertical pump before beginning the process [4-6].

Vertically suspended (VS) pumps and vertical inline pumps are two types of vertical pumps which have been extensively used in a wide range of industrial fields ranging from wastewater sump duties to highly specialized offshore petrochemical industry [5]. Vertically suspended (VS) pumps encompass multiple subgroups, namely vertically suspended diffuser pump (VS1), volute type (VS2), axial flow (VS3), and line shaft (VS4), and cantilever (VS5). VS1 is a vertically suspended, wet pit, radial split, single or multistage, and diffuser pump with a single casing, which discharges liquid through the upright column that suspends the bowl assemblies. VS1 pumps have been broadly utilized in petroleum, petrochemical, chemical, and gas industry process services. A mounting flange can simultaneously couple and support the pump and motor. In general, the application of this type of pump can be cost-effective if installed and maintained properly [7, 8]. Fig.1 shows the schematic drawing of the VS1 pump.

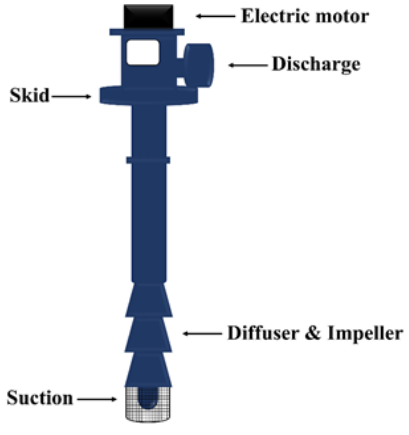

Fig. 1. Schematic illustration of the VS1 pump.

Selecting a desirable material is of significant importance in the construction of a given pump as it ensures its successful performance. The selected material should not only possess favorable resistance to both wear and corrosion but also meet the economic aspect. Cast iron, cast bronze, cast steel, and 300 & 400 series stainless steels have been broadly employed to fabricate the pumps. Among the abovementioned materials, stainless steels have attracted the attention of manufacturers due to their superior properties, such as their high corrosion resistance compared to plain carbon steels [9-13].

The materials selected for fabrication of bolting material for pressure joints should be ASTM, A193 Grade B8M for stainless steel and A193 Grade B7 for carbon steel. Overall, the bolting material should possess adequate corrosion resistance at least equal to that of the impeller.

In the present survey, it is attempted to address the failure mechanism(s) of hex head bolt used in vertically suspended diffuser pump framework using optical microscopy, SEM, XRD, spark-OES, and hardness test. To the best of our knowledge, this is the first report, which evaluates the mechanism(s) involved in the failure of hex head bolt used in vertically suspended diffuser pump framework. Besides, multiple suggestions would be proposed to prolong the service lifetime of the studied bolt.

2. Materials and methods

2.1. Preparation of sample

Fig. 2 schematically presents the configuration of the specific part of the vertically suspended diffuser pump. This part locates at the diffuser and impeller section of the VS1 pump (see Fig. 1).

The as-received failed bolt was cut horizontally to prepare a cross-section for further studies. The optical micrographs of the as-received failed bolt and the prepared cross-section are presented in Fig. 3.

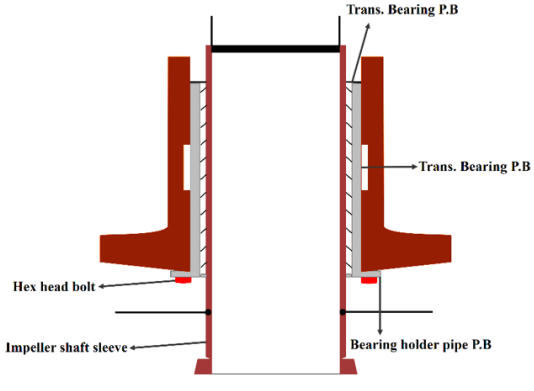

Fig. 2. Schematic representation of the vertically suspended diffuser pump (API VS1 pump) and illustration of the hex head bolt mounting location.

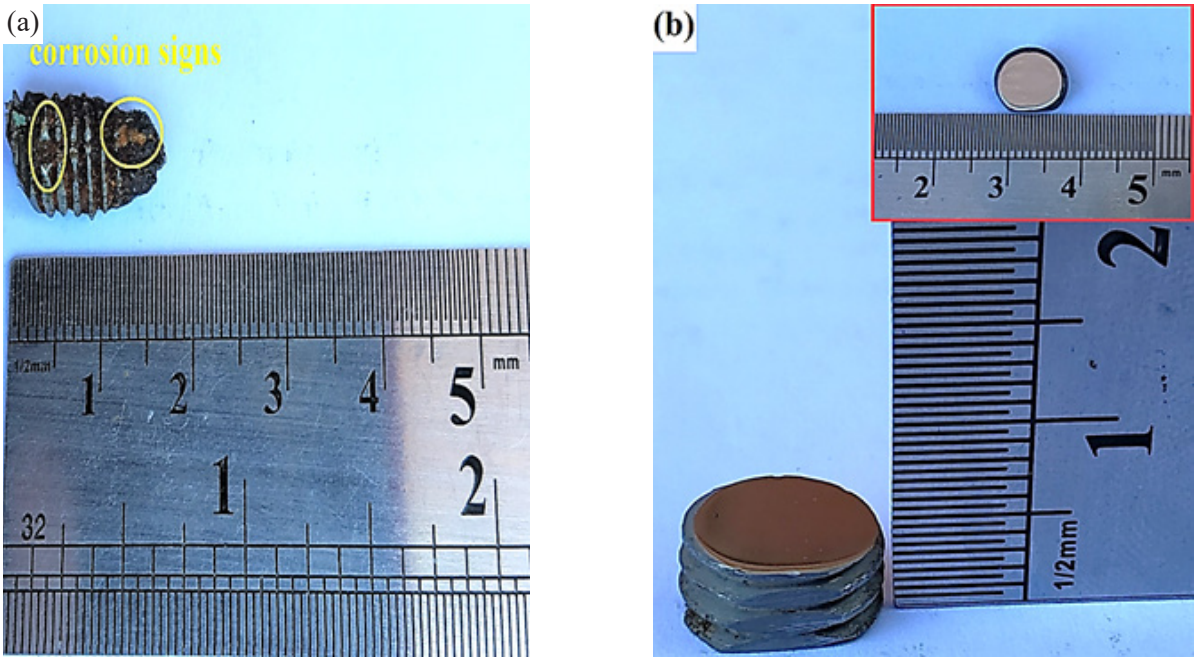

Fig. 3. (a) The optical micrographs of the as-received failed bolt and (b) the prepared cross-section for further investigations.

Fig. 3-a demonstrates that the bolt has been failed from the threaded side. Furthermore, there are corrosion signs on the surface of the failed bolt, as indicated by yellow circles. It worth mentioning that the corrosion attacks have no remarkable contribution to the bolt failure. The failure of the studied bolt not only took the VS1 pump out of service but also caused the failure of the other components of the pump, including split ring and shaft coupling. The prepared cross-section (Fig. 3-b) was mechanically polished using (#80-5000 grit) SiC emery papers followed by a final polishing via 0.3 µm alumina particles to obtain a mirror-like surface finish. For optical microscopy assessment, the polished samples were etched in 4% picral, composing 100 mL ethanol and 4 g picric acid, for 180 s. Fig. 4 exhibits a schematic illustration of the shape and dimensions of hex head bolt. It also shows the failure region. It is advised that the pressure casing bolts should not be less than 0.5 inches in diameter [14].

The surface area of the prepared cross-section was divided into five parts to study and compare the overall properties throughout the surface, as shown schematically in Fig. 5.

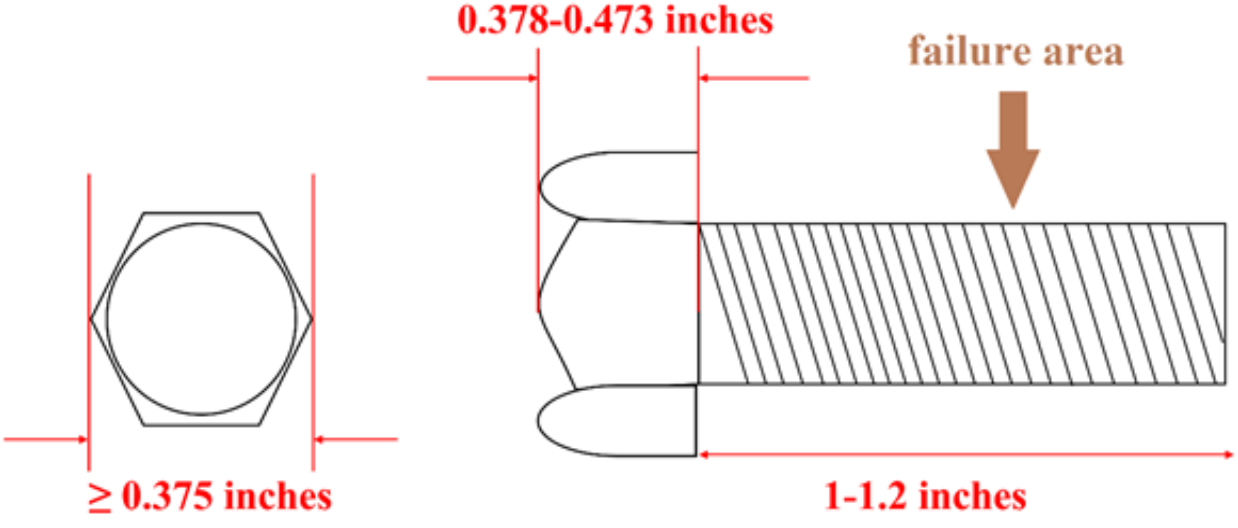

Fig. 4. Schematic illustration of shape and dimensions of hex head bolt, as well as the failure region.

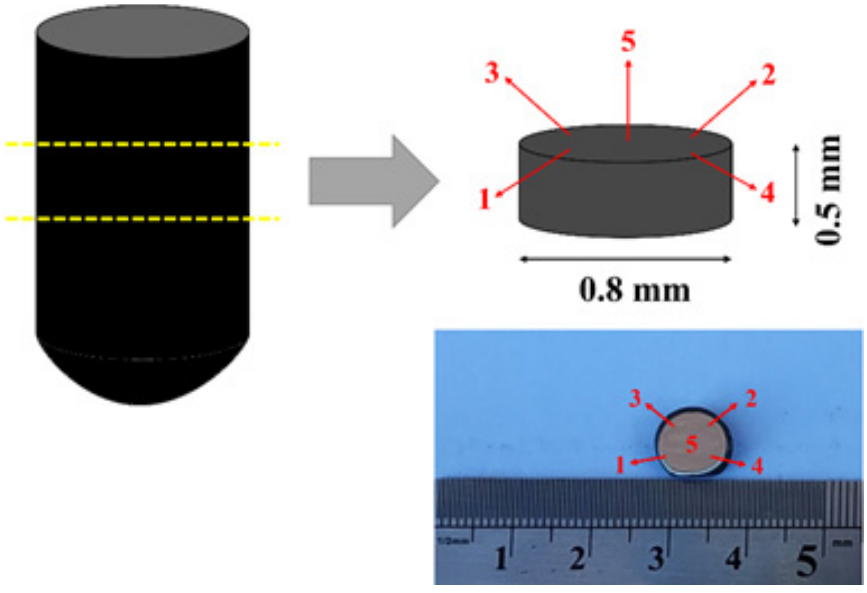

Fig. 5. Schematic illustration of the prepared cross-section that is divided into five parts. These numbers in the following text will denote the different parts of the cross-section.

2.2. Characterization

Spark-optical emission spectroscopy (Spectro-DFS 500, Russia) was employed to reveal the content of constituent elements.

Surface-related properties of the various parts of the failed bolt were assessed using a scanning electron microscope (SEM, Cam scan MV 2200 Vega Tescan, Czech Republic) equipped with an energy dispersive spectrometer (EDS). Besides, the microstructure of the specimens was studied by optical microscopy (OLYMPUS-PMG3, Japan).

The phase structure of the studied bolt was examined by X-ray diffraction (XRD, BRUKER D8 ADVANCE, Germany). Cu Kα radiation with a wavelength of 1.54059 Å was used at a scan range of 2θ=10-120° and a step size of 0.02°.

The microhardness of different regions of the failed bolt was analyzed by M-400-G1/G2/G3 microhardness machine at a load of 100 g for 10 s. The presented results are the average of three different measurements.

3. Results and discussions

3.1. Spark-optical emission spectroscopy

The result of the spark-OES of the cross-section specimen is outlined in Table 1

The obtained result suggests that the hex head bolt is made of X5CrMnN17-8 steel material (1.4154 DIN). This material falls under the classification of stainless steel with high thermal resistance. This alloy has a higher Mn content than that of 316 stainless steel, while its Ni amount is much less than that of 316 stainless steel. The aim behind the addition of Mn to the stainless steel is to increase its mechanical properties. However, the substitution of Ni with Mn has an adverse influence on the corrosion performance of the stainless steel. The poor corrosion resistance of the failed bolt in the present study is ascribed to its high Mn content [15, 16]. The presence of Mn in the microstructure of steel can significantly slow down the critical cooling rate, thereby increasing the hardenability, yield strength, and ultimate strength [17].

It is well accepted that the Cr is the main alloying element in the structure of stainless steel, which guarantees their high corrosion performance in oxidant environments. It also provides a high level of hardenability for the steel, accompanied by promoting its strength and hardness at high temperatures [18-20].

The addition of Ni to the composition of the steel not only enhances its hardenability but also improves the corrosion resistance, where the stainless steel with low Ni may oxidize rapidly. Notably, the amount of Ni in the bolt studied in this work is so low it can cause such a problem [21].

Table 1. The result of the spark-OES from the cross-section of the specimen.

Element	Si	Mn	Cr	Ni	P	C	S	Mo
Content (wt. %)	0.3	8.29	16.7	0.1	0.02	0.086	0.01	0.3

According to the Schaeffler diagram, the microstructure of such a material would be consist of austenite and martensite phases if an appropriate heat treatment is employed.

3.2. Morphological characteristics

The optical micrographs of various parts of the cross-section after polishing are presented in Fig. 6.

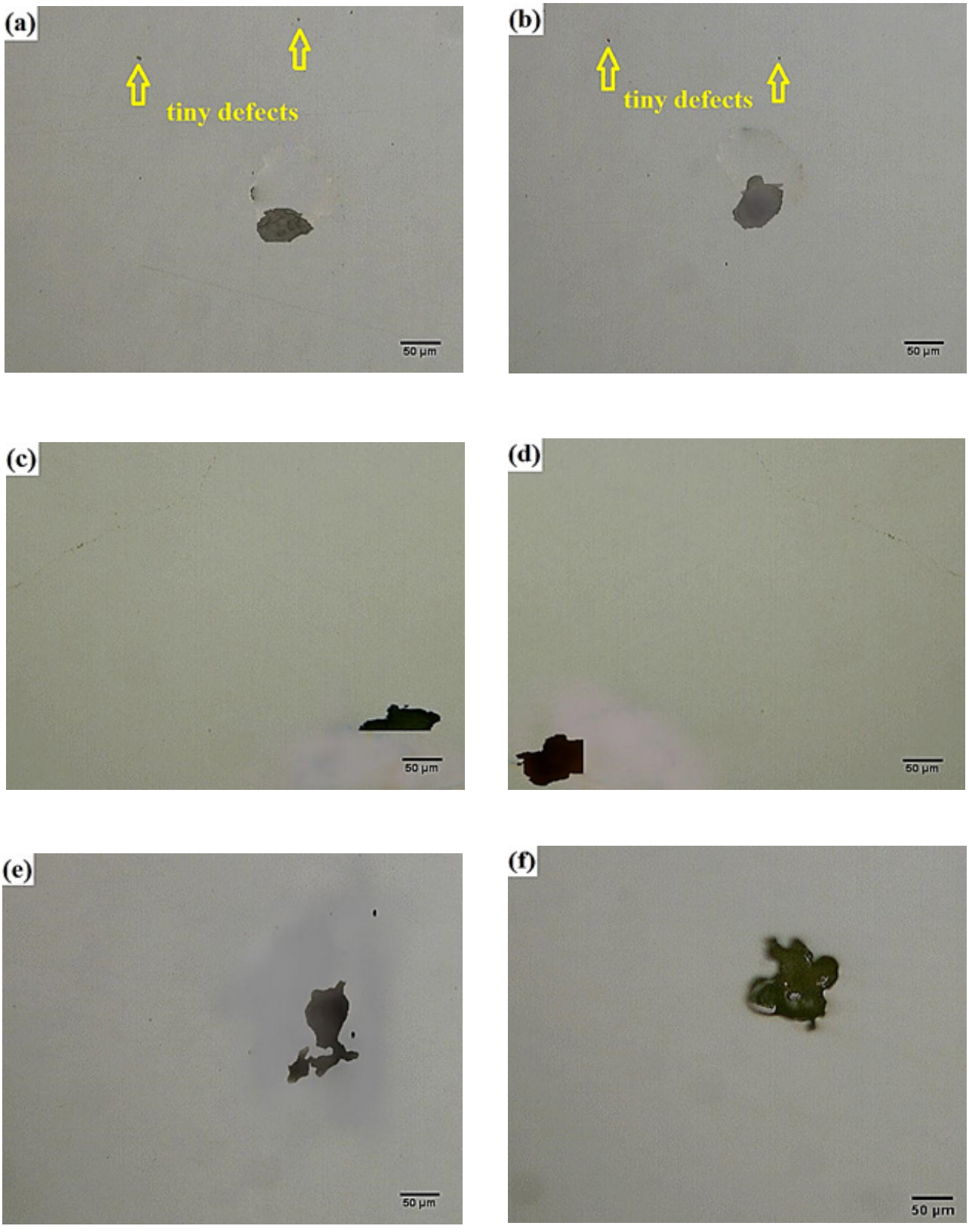

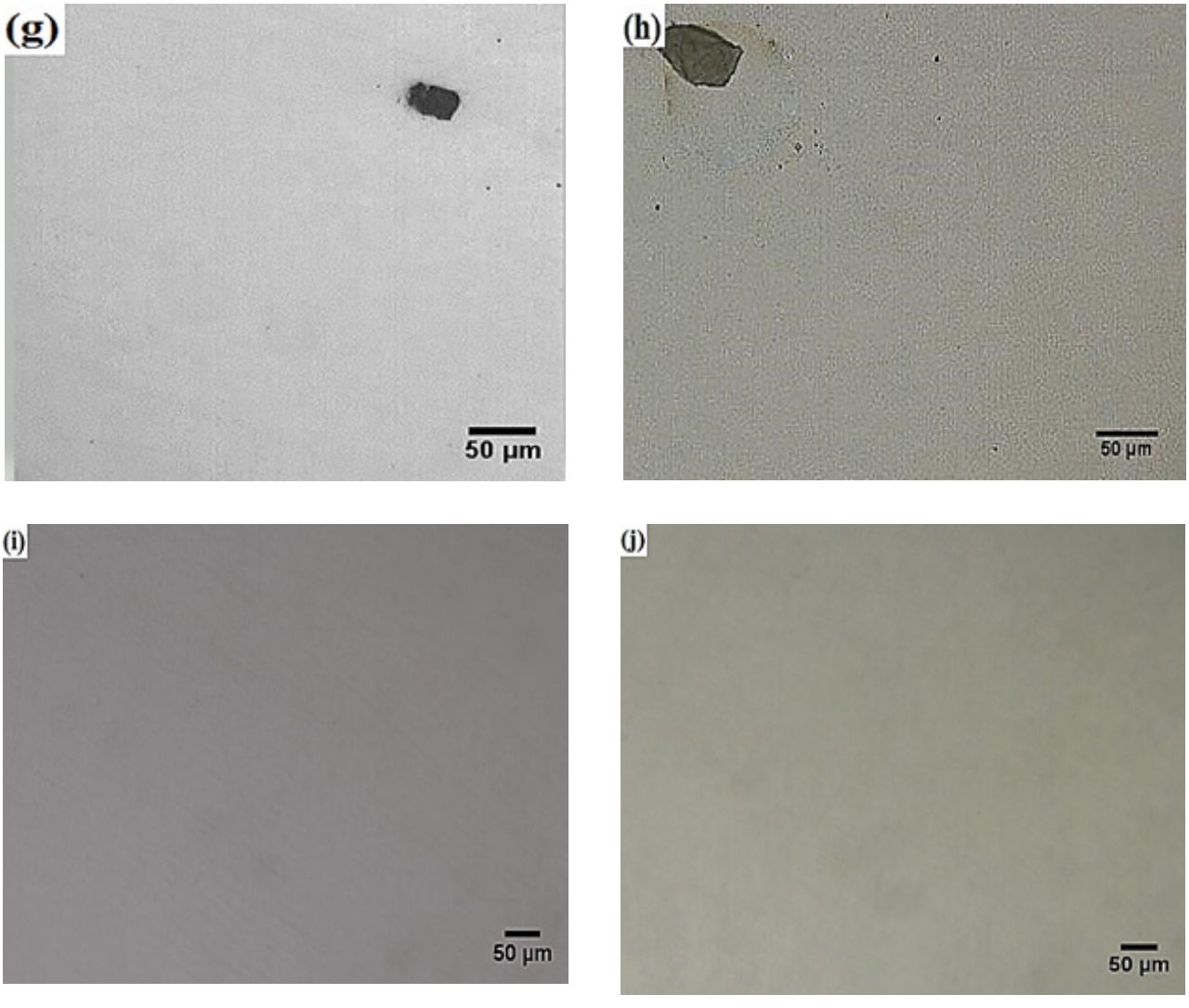

Fig. 6. The optical micrographs of various parts of the cross-section after polishing: (a, b): part 1, (c, d): part 2, (e, f): part 3, (g, h): part 4, and (i and j): part 5.

The obtained micrographs in Fig. 6 (a-h) offer that the parts close to the outer surface of the bolt possess micrometric inclusions that are dispersed over the surface. Furthermore, there can be seen some coarse cavities (50-100 µm) in these parts. Unlike the parts close to the outer surface, a defect-free surface is observable in the central area of the cross-section (see Fig. 6-i and 6). There are a low number of inclusions throughout the microstructure of the studied sample. However, synergistic effects of martensitic structure and large size of the present inclusions (>50 µm) can promote the crack initiation and propagation in the outer surface of the bolt (parts 1-4). Besides these large inclusions, there are also tiny defects observable in OM micrographs (showed by arrows).

The present inclusions in the microstructure of the steels can be originated from different sources, including the molten slag, oxides, and other metallic or non-metallic compounds, which may be formed during the alloying, casting, and post thermal and mechanical processes. On the other hand, the existing pores can be originated within the solidification process due to the decreased solubility of the gases and solidification shrinkage. Since the feeding distance in the casting process of alloying steels is limited compared to carbon steels, a high level of control over the fabrication procedure of these steels is needed to avoid technical problems [22-29]. Fig. 7 shows the etched micrographs of two different parts of the cross-section specimen. In these micrographs, the light and dark phases are corresponded to austenite and martensite, respectively.

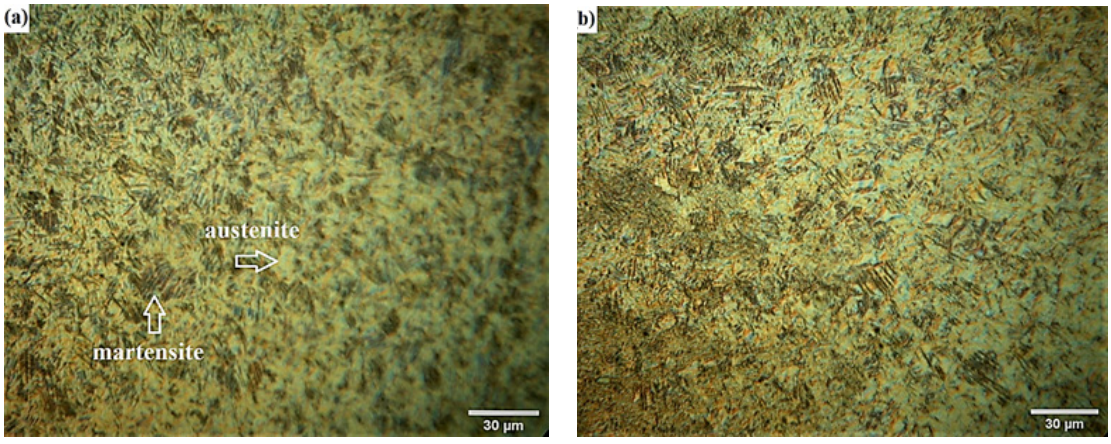

Fig. 7. The etched micrographs of two different parts of the cross-section specimen: (a) part 3 and (b) part 5.

The matrix in both studied parts composed of austenite phase and the martensite blades are dispersed over matrix. A comparison between the presented micrographs demonstrates no remarkable difference in terms of grain size in central and near-surface parts. However, the content of martensite in the outer surface is higher than that of the central part. These findings suggest that controlled thermal and mechanical treatments have been carried out on the bolt, which resulted in a uniform microstructure. SEM images of cross-section specimen at different magnifications are displayed in Fig. 8.

Fig. 8-a shows no defects in the central part of the cross-section, while some defects are formed in the parts close to the outer surface, as shown in Fig. 8-b at the high-resolution.

Turning again to Fig. 6, it seems that some of the observed cavities can be related to probable detachments that occurred around the inclusions. These voids may be generated because of mechanical polishing [30]. Table 2 shows the EDS analysis results of the prepared cross-section.

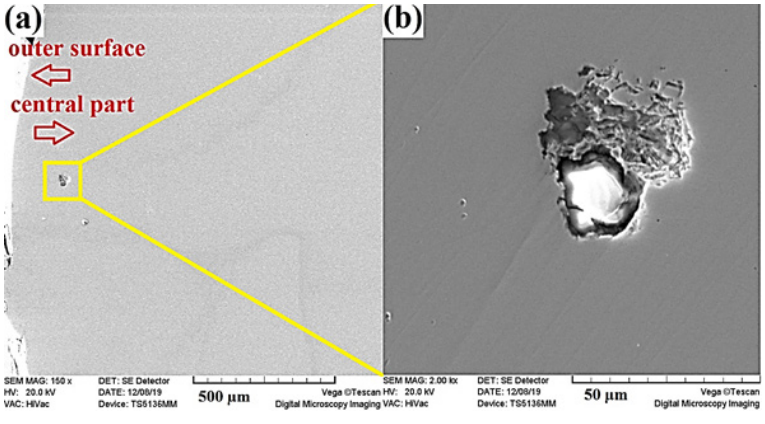

Fig. 8. SEM images of cross-section specimen at different magnifications: (a) 150X and (b) 2000X.

Table 2. EDS analysis results of the prepared cross-section.

Element	Content (wt. %)
Fe	73.0
Cr	14.7
Mn	14.0
Si	0.6

Although EDS is a semi-quantitative method for determining the amount of constituent elements in a given surface [31], the results are well consistent with the spark-OES data except for Mn. EDS data of the inclusion showed in Fig. 8-b is provided in Table 3.

The analyzed inclusion is mainly composed of O, Cr, Fe, S, and Mn elements. It has been demonstrated that different non-metallic inclusions, such as Cr_2O_3, MnS, and SiO_2 can be detected in the structure of the various grades of stainless steels [32]. These undesired compounds may be formed during the alloying process in the melt state. Hence, there should be precise control over the furnace atmosphere, charge materials, and slag removal during the melting process [33].

3.3. Phase analysis

Fig. 9 shows the XRD spectra of the prepared cross-section of the bolt.

The obtained spectrum indicates that the microstructure of the studied specimen contains austenite and martensite phases. The (111), (200), (220), (311), and (222) crystallographic planes of austenite phase as well as (110) plane of martensite at $2\theta=46.6^{o}$ can be seen from the spectra. The results of the XRD spectrum are associated with those obtained from the morphological assay.

Table 3. EDS analysis data of the inclusion showed in Fig. 8-b.

Element	Content (wt. %)
O	52.80
Cr	30.70
Fe	6.60
S	6.14
Mn	2.80
Si	0.88

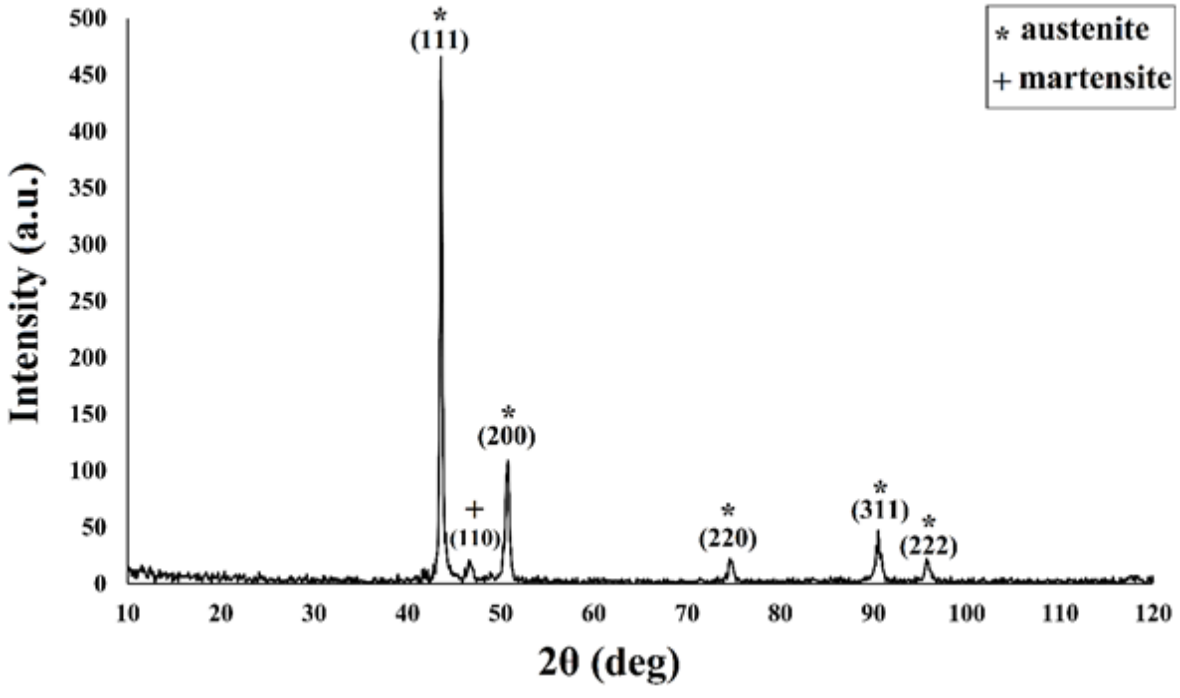

Fig. 9. XRD spectra of the prepared cross-section of the bolt.

3.4. Microhardness

The microhardness values of the various parts of the prepared cross-section specimen are listed in Table 4.

The results clearly demonstrate that the microhardness of the parts close to the surface of the failed bolt is higher than that of the central part, i.e., part 5, mainly due to their higher martensite content [34].

Similar to plain steels, the formation of non-metallic inclusions profoundly degrades the mechanical behavior of the stainless steels. The way that an inclusion alters the mechanical properties of stainless steel intensely depends on its shape and type. For instance, the harder the inclusion, the more the formed microcracks are. The mechanisms that a non-metallic inclusion may affect the mechanical properties of stainless steels are described as follows: (i) **Providing a suitable platform for microcrack formation;** under deformation conditions, a non-metallic inclusion serves as a suitable site for void formation due to the existing mismatch between the thermal and elastic characteristics of the matrix and the inclusion. These voids can further grow and link-up to form microcracks as the deformation proceeds. The formed microcracks act as positions for stress concentration, thereby leading to the failure of the component. (ii) **Fatigue failure;** as mentioned previously, the non-metallic inclusions facilitate the formation of microcracks. Similar behavior is observable under stress cycles which leads to the early fatigue failure of stainless steel. (iii) **Hydrogen embrittlement;** the hydrogen embrittlement within stainless steel can be initiated by entrapping the hydrogen at the inclusions, particularly non-metallic ones [9,35-37].

In this study, the non-metallic inclusions may affect the mechanical properties of the failed bolt through providing a suitable platform for microcrack formation. Meanwhile, the other mentioned factors made a minor contribution.

3.5. Fractography

SEM fractogrpahs of prepared cross-section specimen at two magnifications are presented in Fig. 10.

Table 4. The microhardness values of the various parts of the prepared cross-section.

Studied part	Microhardness (HV)
1	417±13
2	404±8
3	408±10
4	422±5
5	341±4

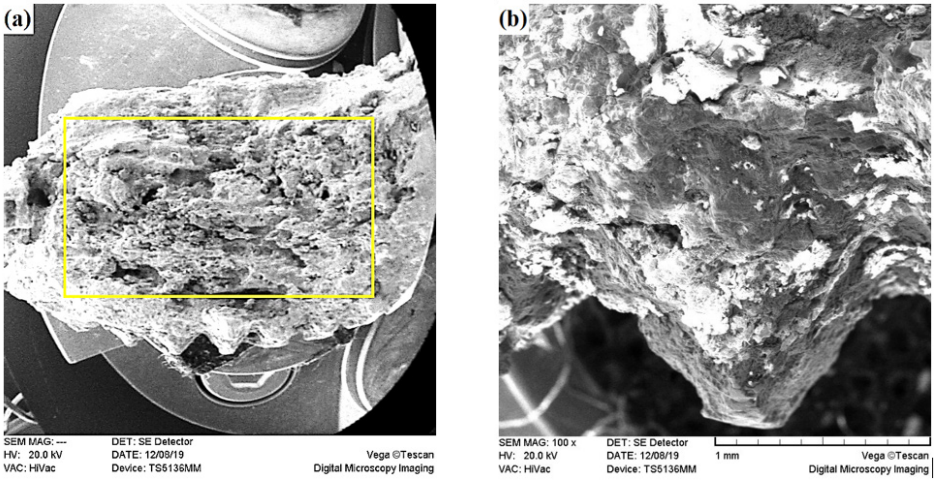

Fig. 10. SEM fractogrpahs of the prepared cross-section specimen at two magnifications: (a) fish-eye image of the entire surface and (b) near-surface brittle fracture image. Yellow Square determines ductile fracture.

As seen in the fish-eye image, it is obvious that there are two different fracture mechanisms at various parts of the specimen. In other words, a flat fracture surface can be observed in parts 1-4, which assigns to brittle fracture. The formed oxide-sulfur duplex inclusions in these parts, namely close to the outer surface and bolt thread, are responsible for cracking in such a failure mechanism. Fig. 10-b provides a high-magnification image of occurred brittle fracture. The central part of the specimen, i.e., part 5, exhibits that ductile fracture has occurred with a sequence of void initiation, propagation, and link-up [38].

4. Conclusions and outlook

This work deals with providing a detailed analysis of the mechanism(s) involved in the early failure of the hex head bolt used in the vertically suspended diffuser pump framework, which has served three years in the marine condition. The failure of the studied bolt not only took the VS1 pump out of service but also caused the failure of the other components of the pump, including split ring and shaft coupling. The main conclusions are as follows: (i) The morphological studies showed a defect-free surface in the central area of the cross-section while the parts close to the outer surface of the bolt possess small inclusions as well as some coarse pores, which may be formed during the alloying, casting, solidification, and post thermomechanical processes. (ii) A survey of the chemical composition of the formed inclusions demonstrated that they mainly contain O, Cr, Fe, S, and Mn elements. (iii) Microstructural characterization indicated that the microstructure of the failed bolt contains austenite and martensite phases where the martensite blades are dispersed over the austenite matrix. (iv) The microhardness of the parts close to the surface of the failed bolt is higher than that of the central part owing to their higher martensite content. (v) Ductile and brittle fracture mechanisms have been observed in the central area and the parts close to the outer surface, respectively. The main parameter that leads to the brittle failure occurrence is attributed to their higher martensite content and formation of oxide-sulfur duplex inclusions.

Besides, some practical suggestions are proposed to prolong the service performance and lifetime of the hex head bolt, as below:

- Controlling the chemical composition of the fabricated bolt to improve the mechanical properties and chemical stability in the service condition. In this case, modification of the chemical composition of the stainless steel by incorporation of Ni may result in promising outcomes as increasing the Ni content of stainless steel can increase its resistance to both corrosion and oxidation.
- Designing a favorable fabrication condition to prevent the generation of pores and oxides in the microstructure of the bolt.
- Tightening-induced tensile stress during the pump mounting should be controlled. It is well known that the synergistic effects of tightening-induced tensile stress and corrosive medium can facilitate the corrosion process. Using the machining technique for bolt threads may lead to a similar problem.
- Surface modification of the fabricated bolt by suitable methods. Notably, the entire surface of the bolt should be uniformly coated by a crack-free coating since pitting and/or localized corrosion may be initiated if there was an un-coated area over the surface.

Reference

[1] T. Agarwal: Int. J. Emerging Technol. Adv. Eng., 2(2012), 163.

[2] A. Nikumbe, V. Tamboli, H. Wagh: Int. Adv. Res. J. Sci. Eng. Technol., 2(2015), 117.

[3] P. Ganesh, S.R. Krishna: J. Fail. Anal. Prev., 20(2020), 1019.

[4] R. Birajdar, A. Keste: J. Vib. Eng. Technol., 8(2020), 417.

[5] M. Volk: Pump characteristics and applications, CRC Press, Boca Raton, (2013), 1.

[6] R. Achouri, O. Nouicer, H. Mhiri, P. Bournot: Eng. Fail. Anal., 29(2013), 1.

[7] M. Mohammadzadeh, M. Arbabtafti, M. Shahgholi: Arch. Appl. Mech., 89(2019), 245.

[8] S. Agnihotri, P. Gautam: IJSRD, 3(2015), 2321.

[9] J.H. Park, Y. Kang: Steel Res. Int., 88(2017), 1700130.

[10] R. Merello, F.J. Botana, J. Botella, M.V. Matres, M. Marcos: Corros. Sci., 45(2003), 909.

[11] R. Corbett, F. Sherman: J. Fail. Anal. Prev., 5(2005), 8.

[12] S. O. A. B. A.Obadele, F.V. Adams: J. Fail. Anal. Prev., 20(2020), 833.

[13] W. Guo, N. Ding, L. Liu, N. Xu, N. Li, F. Zhang, L. Chen: J. Fail. Anal. Prev., 20(2020), 483.

[14] API Standard: American Petroleum Institute, (2010).

[15] I.H. Toor: J. Chem., 2014(2014), 1. https://doi.org/10.1155/2014/951471

[16] B. Kim, S. Kim, H. Kim: Adv. Mater. Sci. Eng., 2018(2018), 1. https://doi.org/10.1155/2018/7638274

[17] G. Niu, H. Wu, D. Zhang, N. Gong, D. Tang: Mater. Sci. Eng. A., 725(2018), 187.

[18] S.S. Tavares, R.T. Batista, R.V. Landim, J.A. Velasco, L. Senna: Eng. Fail. Anal., 113(2020), 104553.

[19] Y.J. Kim, S.W. Kim, H.B. Kim, C.N. Park, Y.I. Choi, C.J. Park: Corros. Sci., 152(2019), 202.

[20] C.R. Anoop, A. Prakash, S.K. Giri, S.N. Murty, I. Samajdar: Mater. Charact., 141(2018), 97.

[21] H. Zhang, C.H. Zhang, Q. Wang, C.L. Wu, S. Zhang, J. Chen, A.O. Abdullah: Opt. Laser Technol., 101(2018), 363.

[22] M. Kiviö, L. Holappa: Metall. Mater. Trans. B., 43(2012), 233.

[23] R. Atwood, P. Lee: Metall. Mater. Trans. B., 33(2002), 209.
[24] G. Marami, M.S. Safavi, M.A.S. Sadigh: J. Cent. South Univ., 25(2018), 561. https://doi.org/10.1007/s11771-018-3761-4
[25] S. Ou, K.D. Carlson, R.A. Hardin, C. Beckermann: Metall. Mater. Trans. B., 33(2002), 741.
[26] S. Xu, Y.Z. Liu, L.Y. Zhou, Y.M. Yan, H.W. Zhu: J. Fail. Anal. Prev., 14(2014), 183.
[27] M.F. Tayyebi, F. Ghanbari, A. Kumar: IJISSI, 15(2018), 49.
[28] A. Abyaziand, A. Ebrahimi: IJISSI, 11(2015), 1.
[29] A. Homayoun, M. Shahmohammadi, M. Soltanieh, A. Afzali: 3(2006), 29.
[30] M. Koopaie, A. Bordbar-Khiabani, S. Kolahdooz, A.K. Darbandsari, M. Mozafari: Mater. Res. Express, 7(2020), 015417.
[31] J.L. Weaver, J. Reiser, O.K. Neill, J.S. McCloy, N.A. Wall: MRS Online Proceedings Library (OPL), 1744(2014), 101.
[32] C. Mapelli, P. Nolli: ISIJ Int., 43(2003), 1191.
[33] M. Etminanfar, M.S. Safavi, N. Abbasian-Vardin: Eng. Fail. Anal., 112(2020), 104533.
[34] A. Rehman, Y. Liang, M.H. Bidabadi, Z. Yu, C. Zhang, H. Chen, Z.G. Yang: J. Iron. Steel. Res. Int., 26(2019), 1069.
[35] E.Y. Guo, M.Y. Wang, T. Jing, N. Chawla: Mater. Sci. Eng. A., 580(2013), 159.
[36] A.L. Vasconcellos da Costa e Silva: JMR&T., 8(2019), 2408.
[37] B.G. Bartosiaki, J.A. Pereira, W.V. Bielefeldt, A.C. Vilela: J. Mater. Res. Technol., 4(2015), 235.
[38] R. Garber, I. Bernstein, A. Thompson: Metall. Mater. Trans. A., 12(1981), 225.